group of **2** appeared at δ 1.20. Addition of $Eu(fod)_3$ caused the downfield resonance at δ 1.62 to separate; the resonance that moved more rapidly downfield depended on the composition of the diazene mixture and the amount of shift reagent added. Identification of **1** and **2** was achieved by comparison of the spectra with those of known $Eu(fod)_3$-treated mixtures.

Control experiments showed that the isolation procedures caused no change in the composition of a known **1/2** mixture.

Quantitative analysis of the **1/2** ratio was achieved by integration of the bridged methyl peak and the downfield fused methyl peak. The average of 50 integrations was taken for each sample. Table IV gives the results.

Test for Rearrangement in the Photolysis of Bridged Diazene 1. A similar set of samples of **1** in CH_3CN solution was irradiated at 0 °C for various extents of deazetation (5–95% conversion) in a Rayonet reactor. The diazene recovered from each sample was analyzed by the above technique and found to contain no fused diazene **2**.

Kinetic analysis of the rearrangement and deazetation was aided by the use of an interactive computer program, kindly provided by Professor Martin Saunders and modified for use with the PDP-1145 computer by Dr. B. K. Carpenter, to whom we are indebted. A subroutine of the differential rate equations corresponding to the triangular scheme of Eq 1 was written, and the program was given trial rate constants and initial concentrations as input data. The program used a Runge–Kutta scheme to integrate the differential equations. Graphs of the fit of the experimental points to the calculated curves are shown elsewhere.[9b]

Product Distribution Studies. The data of Figure 1 were obtained by techniques similar to those described elsewhere.[8]

Acknowledgment. We thank the National Science Foundation (CHE 76-00416) and the National Institute of General Medical Sciences (GM-23375) for grants in support of this work.

Mechanistic Aspects of the Electrochemical Oxidation of Dihydronicotinamide Adenine Dinucleotide (NADH)

Jacques Moiroux and Philip J. Elving*

Contribution from the Ecole Normale Superieure de l'Enseignement Technique, 94230 Cachan, France, and Department of Chemistry, University of Michigan, Ann Arbor, Michigan 48109.
Received February 4, 1980

Abstract: The apparently single stage anodic oxidation of NADH involving removal of two electrons and a proton to form NAD^+ has been examined with particular attention to the deprotonation step and its relationship to the initial potential-determining electron-transfer step, primarily at glassy carbon electrodes (GCE) in aqueous media with supplementary studies at pyrolytic graphite and platinum electrodes in aqueous media and at GCE in Me_2SO; the carbon electrodes were generally first covered with an adsorbed NAD^+ layer in order to eliminate adsorption-controlled faradaic processes. The initial step is an irreversible heterogeneous electron transfer (transfer coefficient $\beta = 0.37$ at carbon electrodes and 0.43 at platinum). The resulting cation radical $NAD{\cdot}H^+$ loses a proton (first-order reaction; rate constant k) to form the neutral radical NAD· which may participate in a second heterogeneous electron transfer (ECE mechanism) or in a homogeneous electron transfer with $NAD{\cdot}H^+$ (disproportionation mechanism DISP 1 or half-regeneration mechanism), yielding NAD^+. The near identities of current functions, viscosity-corrected diffusion coefficients D and β values, point to essentially similar solute species and charge-transfer paths being involved in different media and at different electrodes. D is ca. 2×10^{-6} cm^2 s^{-1} in aqueous solution; k is ca. 60 s^{-1} at the GCE covered with adsorbed NAD^+.

The grossly reversible redox behavior exhibited by the $NAD^+/NADH$ couple under physiological conditions

$$NAD^+ + H^+ + 2e^- \rightleftharpoons NADH \quad (1)$$

has prompted extensive electrochemical study of the reaction. Although polarographic or voltammetric reduction of nicotinamide adenine dinucleotide (NAD^+, DPN^+, coenzyme I) has been extensively investigated, there are only a few systematic studies of the voltammetric oxidation of 1,4-dihydronicotinamide adenine dinucleotide (NADH).[1-4]

Currently, there is increasing interest in the electrochemical oxidation of NADH (cf. ref 5 and 6 for summaries of recent studies) from the viewpoints of (a) analysis, e.g., in determining compounds which react under enzymatic conditions with NAD^+ to produce NADH, (b) using electrochemical approaches and methodology to study biological systems and phenomena, e.g., importance of the $NAD^+/NADH$ couple in the electron-transport chain, and (c) using one direction of the $NAD^+/NADH$ couple as an electrochemical regeneration step in cyclic redox processes involving chemical transformation and/or energy conversion.

In both aqueous and nonaqueous media, NADH shows a single diffusion-controlled cyclic voltammetric anodic peak; scan reversal produces a cathodic peak due to NAD^+. A cathodic peak complementary to the anodic peak, as expected for a reversible redox couple, was not seen at the highest scan rates used (50 V s^{-1} in aqueous media, 10 V s^{-1} in nonaqueous media).

Since mercury is oxidized at the positive potentials at which NADH gives its anodic signal, electrodes of materials such as carbon or platinum must be used. The generally easier oxidation of NADH at carbon (commonly, pyrolytic graphite or glassy carbon) than at platinum electrodes is of general interest because the pronounced increase in background current at both carbon and platinum electrodes makes it difficult to obtain a well-defined limiting current, especially at low NADH concentrations. The increase in background current at platinum starting at 0.5 V can be explained by surface oxide formation; the cause for the background current increase at carbon starting at 0.6 V is uncertain.

Although there has often been a failure to oxidize NADH cleanly at solid electrodes, it is well established that it undergoes a two-electron (2e) oxidation to yield the corresponding enzymatically active nicotinamide (NAD^+).[6-9] However, there is still

*To whom correspondence should be addressed at the University of Michigan.

(1) A. L. Underwood and R. W. Burnett in "Electroanalytical Chemistry", Vol. 6, A. J. Bard, Ed., Marcel Dekker, New York, 1972, Chapter 1.
(2) P. J. Elving, C. O. Schmakel, and K. S. V. Santhanam, *CRC Crit. Rev. Anal. Chem.*, **6**, 1 (1976).
(3) P. J. Elving, *Top. Bioelectrochem. Bioenerg.*, **1**, 276 (1976).
(4) G. Dryhurst, "Electrochemistry of Biological Molecules", Academic Press, New York, 1977.
(5) J. Moiroux and P. J. Elving, *Anal. Chem.*, **50**, 1096 (1978).
(6) R. D. Braun, K. S. V. Santhanam, and P. J. Elving, *J. Am. Chem. Soc.*, **97**, 2591 (1975).
(7) W. J. Blaedel and R. A. Jenkins, *Anal. Chem.*, **47**, 1337 (1975).
(8) P. Leduc and D. Thevenot, *Bioelectrochem. Bioenerg.*, **1**, 96 (1974); P. Leduc and D. Thevenot, *J. Electroanal. Chem.*, **47**, 543 (1973).

0002-7863/80/1502-6533$01.00/0

Table I. Oxidation of NADH at Glassy Carbon, Pyrolytic Graphite, and Platinum Electrodes

Voltammetry at the RDE (10 rps; $v = 2$ mV s^{-1})[a]

electrode	$E_{1/2}$, mV	i_l/AC, μA cm^{-2} mM^{-1}	$dE/d(\log [i/(i_l - i)])$, mV	βn_a
GCE[b,c]	450 ± 10[e]	295 ± 3	160 ± 5	0.37 ± 0.01
PGE[b,d]	520 ± 10	300 ± 3	167 ± 2	0.360 ± 0.005
PE[d]	510 ± 10	290 ± 10	137 ± 4	0.43 ± 0.03
GCE[b,i]	610 ± 10	103 ± 5	167 ± 5	0.36 ± 0.01

Voltammetry at the Stationary Electrode ($v = 0.05$ V s^{-1})[a]

electrode	E_p, mV	$E_{p/2}$, mV	$i_p/ACv^{1/2}$, μA cm^{-2} mM V$^{-1/2}$ s$^{1/2}$	βn_a[f] $= 1.857RT/F(E_p - E_{p/2})$	βn_a[g]
GCE[b,c]	475 ± 10	345 ± 10	493 ± 8	0.37 ± 0.01	0.35 ± 0.03
PGE[b,d]	560 ± 15	425 ± 10	490 ± 10	0.36 ± 0.01	0.38 ± 0.03
PE[d]	550 ± 20	440 ± 15	420 ± 20[h]	0.40 ± 0.03	0.45 ± 0.03

[a] Currents are corrected for background currents. NADH concentration = 1 mM. [b] Electrode covered with adsorbed NAD^+. [c] Background: 0.5 M KCl or 0.25 M K_2SO_4; 0.05 M Tris or phosphate buffer; pH ≥7. Data given are the mean and standard deviations for 10 experiments. [d] Background: 0.5 M KCl; 0.05 M Tris buffer; pH 7.1. Data given are the mean and standard deviations for 5 experiments. [e] Independent of NADH concentration between 0.5 and 2 mM. [f] Equation is discussed in ref 17. [g] Determined graphically from a plot of E_p vs. $\log v$ (cf. Figure 2) since $dE_p/d(\log v) = (29.6/\beta n_a)$ mV.[13] [h] Diffusion-controlled current function, calculated from eq 2 with $\beta n_a = 0.43$ and $D = 2 \times 10^{-6}$ cm^2 s^{-1}, is 560. [i] Background: 0.1 M Bu_4NClO_4 in Me_2SO. Data given are the mean and standard deviations for 3 experiments.

considerable uncertainty about the details of the reaction path. The present paper describes the use of a variety of electrochemical approaches to reveal some such details, especially in respect to the deprotonation step and its relation to the initial potential-determining electron-transfer step.

Experimental Section

Unless otherwise indicated, procedures and other experimental details were identical with those previously described.[5]

Chemicals. NADH and NAD^+ (P-L Biochemical Chromato-Pure Grade), 2-amino-2-methyl-1,3-propanediol (Tris) (Sigma), tetra-*n*-butylammonium perchlorate (G. Frederick Smith), dimethyl sulfoxide (Me_2SO) (Fisher), and reagent grade chemicals (Baker) were used.

Electrodes. The working electrodes were used in stationary and rotating disk configurations. The glass carbon electrodes (GCE) were those previously designated as GC-1 and GC-2[5] (area = 0.230 cm^2 for GC-1 and 0.254 cm^2 for GC-2). The pyrolytic graphite electrode (PGE) was also previously described[5] (area = 0.383 cm^2) as was the platinum electrode (PE)[10] (area = 0.0090 cm^2). A Tacussel EDI rotating glassy carbon electrode was used to examine the effect of angular viscosity.

The reference electrode was an aqueous saturated calomel electrode, to which all potentials cited are referred; potentials cited are for reduction half-cells. The counter electrode was a platinum gauze.

Electrode Pretreatment. A working carbon electrode designated as *pretreated* or *clean* before being used was conditioned (15 sweeps from 1.50 to −1.50 V at 0.1 V s^{-1}) and pretreated (1.50 V for 2 min, −1.50 V for 2 min, repeated twice) in the background solution (water or Me_2SO as solvent), following Blaedel and Jenkins.[11] Background cyclic voltammograms (0.00–0.75 V, scan rate = 2 mV s^{-1}) were then recorded at the rotating disk electrode (RDE) until successive cycles yielded superposable curves; NADH solution was added, and the electrode, held at the initial potential of 0 V, was rotated for 2 min before recording each voltammetric curve. Pretreatment between experiments on the same NADH solution was unnecessary. Between experiments on different NADH solutions, the electrode was rinsed with distilled water, wiped with a paper tissue, and stored while immersed in distilled water.

A *covered* electrode, i.e., one coated with adsorbed NAD^+,[10,12] was prepared by being held at 0.75 V while rotated in 1 mM NADH solution for 1 h. Reproducible results are obtained with such an electrode by rinsing it with distilled water and storing it in the air when not in use; when used, the electrode, held at 0 V, is rotated for 2 min before recording each voltammetric curve (cf. ref 10 for details concerning electrode preparation and use).

Each new working carbon electrode was first conditioned and pretreated and then used as either a clean or a covered electrode.

The only pretreatment of the PE necessary to obtain reproducible voltammetric curves is to rotate it, held at the initial potential of 0.0 V, for 2 min before each scan.

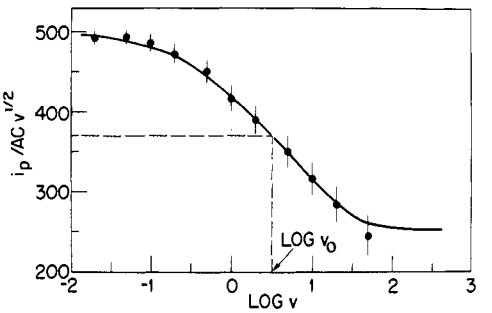

Figure 1. Variation of the voltammetric peak current function, $i_p/ACv^{1/2}$, with scan rate, v, at a stationary "covered" GCE, corrected for background current (i_p in μA, A in cm^2, C in mM, v in V s^{-1}). Solution composition: 1 mM NADH, 0.5 M KCl, 0.05 M Tris buffer; pH 7.1. Experimental margins of errors are represented for each measurement. The continuous curve is computed by using the working curve given in ref 13 for $k = 60$ s^{-1} in the case of an ECE mechanism since $RTk = \beta Fv_0$.

Apparatus. Electrochemical measurements were made with a Princeton Applied Research 170 multipurpose instrument and a three-compartment water-jacketed cell, whose counter and reference electrode compartments were filled with the background solution and whose temperature, unless otherwise specified, was 25 °C. For cyclic voltammetry and potential-step chronoamperometry, a Tekronix 5103N cathode ray oscilloscope with suitable modules and cameras was used. A Sargent synchronous motor (10 revolutions/s) was used to rotate the electrode except for data recorded in Table II. A Tacussel Controvit servocontrol electronic amplifier was used in connection with the Tacussel GCE.

Results and Discussion

Past papers[5,10,12] on the electrolytic oxidation of NADH have described the effect of experimental conditions in producing a voltammetric prewave or prepeak as a result of adsorption at the solution/electrode interface of NAD^+ produced in the oxidation, as well as the adsorption phenomena involved and procedures for avoiding the overlapping waves or peaks due to the presence of both adsorption-controlled and diffusion-controlled processes, by suppressing the current due to production of adsorbed NAD^+ through the use of a covered carbon electrode, i.e., one which has a tightly adhering adsorbed layer of NAD^+ on its surface.

Behavior at a Glassy Carbon Electrode. Unless otherwise indicated, behavior ascribed to a GCE was obtained at the covered GC-2 electrode. Current and potential reproducibility for oxidation of 0.005–1 mM NADH are excellent.[5,10]

Characteristics of the anodic NADH wave or peak at rotating and stationary electrodes are summarized in Table I.

Results on single-sweep voltammetry at high scan rate (v) at the stationary electrode are independent of pH and background electrolyte composition. A single peak corresponding to an ir-

(9) R. W. Coughlin and B. F. Alexander, *Biotechnol. Bioeng.* **17**, 1379 (1975).
(10) J. Moiroux and P. J. Elving, *Anal. Chem.*, **51**, 346 (1979).
(11) W. J. Blaedel and R. A. Jenkins, *Anal. Chem.*, **46**, 1952 (1974).
(12) J. Moiroux and P. J. Elving, *J. Electroanal. Chem.*, **102**, 93 (1979).

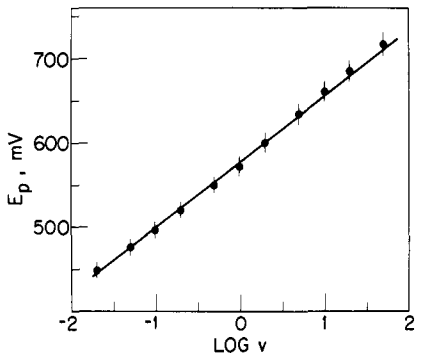

Figure 2. Variation of the voltammetric peak potential E_p with scan rate. Conditions are the same as in Figure 1.

reversible process is recorded; no peak due to an adsorption-controlled process appears.[12] The peak current function, $i_p/ACv^{1/2}$, which is approximately constant at v less than 0.1 V s^{-1}, decreases continuously as v increases (Figure 1), showing that a relatively slow chemical step is involved in the electrochemical process.

The peak potential E_p exhibits a positive linear shift with increasing log v (Figure 2) while the difference $E_p - E_{p/2}$ remains approximately constant ($E_{p/2}$ is the half-peak potential).

Characteristics of the wave and peak, when they seemingly correspond to a diffusion-controlled process ($v \leq 0.1$ V s^{-1}), are given in Table I. Values of βn_a obtained at the RDE and stationary electrode coincide; β is the transfer coefficient for the potential-determining heterogeneous electron transfer and n_a is the number of electrons involved in that step (generally one) so that $dE/d(\log [i/(i_l - i)]) = 2.3RT/\beta n_a F$.

The single-sweep voltammetric data fit the Saveant criteria[13] for an ECE mechanism[14] where the first step is rate limiting and the chemical step is also relatively slow so that a 2e process is observed at slow sweep rate v and a 1e process tends to be observed at fast v. In Saveant's nomenclature,[13] a change from an IR-1 reaction scheme where a 1e process is kinetically controlled by the electron transfer to an IE-2 reaction scheme where a 2e irreversible process is kinetically controlled by the first electron transfer is observed as v decreases.

On potential-step chronoamperometry at the stationary electrode, the variation of i with $t^{-1/2}$ (Figure 3) is linear only at $t^{-1/2}$ less than 3 ($di/d(t^{-1/2}) = 42.5$ μA $s^{1/2}$). When $t^{-1/2}$ exceeds 3, i is less than calculated from this linear relation; the difference increases with increasing $t^{-1/2}$.

In an ECE mechanism, as a result of the transition from a 2e to a 1e process, i should tend to the value given by the straight line with a slope of 21.75 μA $s^{1/2}$ in Figure 3 at large $t^{-1/2}$.[15] Figure 3 shows that this may be the case within the experimental margin of error.

Behavior at a Pyrolytic Graphite Electrode. Characteristics of voltammetric curves recorded with the covered PGE[10,12] are given in Table I. Although oxidation of NADH at PG is appreciably more difficult than at GC, the near identity of the current functions for both types of carbon support identical control of the faradaic processes involved; the near identity of the βn_a products point to identical controlling mechanistic steps being involved.

Behavior at a Platinum Electrode. No evidence for an adsorption-controlled process was seen at rotating or stationary platinum electrodes.

At pH 7.1, a well-defined wave is obtained with the platinum RDE,[10] whose $E_{1/2}$ is close to that at the PGE but whose slope is greater; consequently, βn_a is greater at the PE than at carbon electrodes. E_p on sweep voltammetry at the stationary PE is close to that at the PGE; the current function never reaches the value

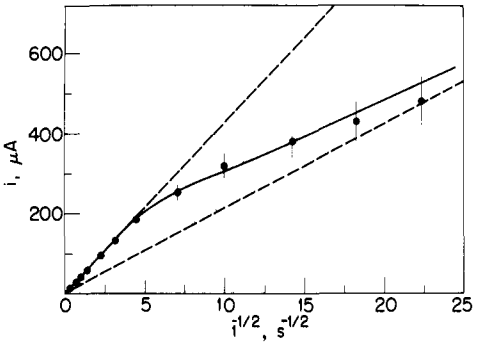

Figure 3. Variation of the current with time (t) on potential-step chronoamperometry at a stationary covered GCE, corrected for background current. Solution composition: 1 mM NADH, 0.5 M KCl, 0.05 M Tris buffer; pH 7.1. Initial potential = 0.1 V; final potential = 0.7 V. The dotted lines represent slopes of 42.50 and 21.75 μA $s^{1/2}$. Experimental margins of errors are represented for each measurement. The continuous curve is computed by using the relation $i = FACD^{1/2}[2 - \exp(-kt)]/(\pi t)^{1/2}$ [15]

corresponding to a purely diffusion-controlled process (Table I), even at v as slow as 0.01 V s^{-1}. However, the current function magnitude at the RDE is comparable to those at rotating carbon electrodes.

Between pH 6 and 8 with KCl as supporting electrolyte or Na_2SO_4 at pH above 7, the voltammetric parameters ($E_{1/2}$, i_l/AC, and wave slope at the RDE; E_p, $E_{p/2}$, and $i_p/ACv^{1/2}$ at the stationary PE) do not change appreciably. Above pH 8, the current–potential curves at both RDE and stationary PE become less well-defined as pH increases, as previously reported.[10]

Oxidation in Me_2SO. The oxidation of NADH (1 mM) in Me_2SO (0.1 M in tetra-*n*-butylammonium perchlorate) at the GC-2 electrode was examined primarily to see if the change in solvent affected the states of NADH and intermediary species or the nature of the electron-transfer reaction.

The originally clean electrode surface is largely occupied by adsorbed Bu_4N^+ ions, which minimizes adsorption of NAD^+ generated by the NADH oxidation.[12] However, if the RDE is held at a potential at which NADH is oxidized, $E_{1/2}$ for the NADH anodic wave, as in aqueous media, slowly becomes more positive, indicating coverage of the electrode surface with NAD^+ adsorbed in the tenaciously held perpendicular orientation which may displace—at least partially—Bu_4N^+ ions.

$E_{1/2}$ at the RDE (covered with adsorbed NAD^+ by holding the electrode at 0.8 V for 2 h) is 610 ± 10 mV compared to 450 ± 10 mV in aqueous media, but the wave slope and βn_a product are the same; i.e., $\beta n_a = 0.36 \pm 0.01$ in Me_2SO and 0.37 ± 0.01 in water (Table I). The latter result supports essentially similar charge-transfer paths in the two solvents.

Diffusion Coefficient of NADH. On potential-step chronoamperometry at the covered GCE, the diffusion coefficient of NADH can be calculated by the Cottrell equation[16] from the variation of i with $t^{-1/2}$ (Figure 3), when linear and corresponding to a 2e process. For 1 mM NADH, $D = (2.3 \pm 0.1) \times 10^{-6}$ cm^2 s^{-1} in 0.5 M KCl plus 0.05 M Tris buffer (pH 7.1) and $(2.1 \pm 0.1) \times 10^{-6}$ cm^{-2} s^{-1} in 0.25 M Na_2SO_4 plus 0.05 M phosphate buffer (pH 9.1) (mean and standard derivations for five experiments in each case).

D may also be evaluated from the characteristics of the voltammetric peak at the stationary GCE (Table I), by using eq 2 for an irreversible 2e transfer.[17] The result, $(1.9 \pm 0.1) \times 10^{-6}$ cm^{-2} s^{-1}, is compatible with those calculated from potential-step chronoamperometry and that previously reported ($D = 2.4 \times 10^{-6}$ cm^2 s^{-1}).[18]

$$i_p/ACv^{1/2} = (602 \times 10^3)0.496n(\beta n_a)^{1/2}D^{1/2} \quad (2)$$

(13) L. Nadjo and J. M. Saveant, *J. Electroanal. Chem.*, **48**, 113 (1973).
(14) In describing electrochemical reaction mechanisms, C refers to a chemical reaction step and E refers to an electron-transfer step; thus, ECE refers to a sequence of two electron-transfer steps with an intervening chemical reaction.
(15) G. S. Alberts and I. Shain, *Anal. Chem.*, **35**, 1859 (1963).
(16) F. G. Cottrell, *Z. Phys. Chem., Stoechiom. Verwandschatsl.*, **42**, 385 (1902).
(17) R. S. Nicholson and I. Shain, *Anal. Chem.*, **36**, 706 (1964).
(18) M. Aizawa, R. N. Coughlin, and M. Charles, *Biochim. Biophys. Acta*, **385**, 362 (1975).

Scheme I

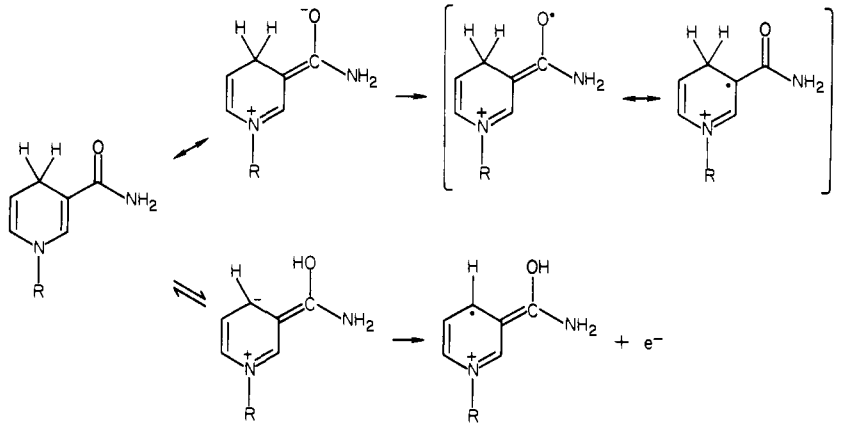

(8a)

(8b)

For 1 mM NADH, the ratio of the limiting plateau currents obtained at the RDE in Me_2SO and water is $i_{p(Me_2SO)}/i_{p(H_2O)} = 0.35 \pm 0.02$. When there is no marked difference in solvation between solvents, the ηD product for a solute is constant (η is the solvent viscosity; D is the diffusion coefficient of the solute in the given solvent). Since the limiting current is given[19] by eq 3, where

$$i_p = nFAC\omega^{1/2}D^{2/3}/1.62\nu^{1/6} \quad (3)$$

ω is the angular rotation speed of the electrode and ν is the kinematic viscosity of the solvent (product of its viscosity and density (d)), and since the same electrode rotated at the same angular speed was used in both solvents, relation (4) applies, where $d_{H_2O} = 0.997$ g/cm^3 and $d_{Me_2SO} = 1.096$ g/cm^3 at 25 °C.

$$i_{p(Me_2SO)}/i_{p(H_2O)} = (D_{Me_2SO}/D_{H_2O})^{5/6}(d_{H_2O}/d_{Me_2SO})^{1/6} = 0.985(D_{Me_2SO}/D_{H_2O})^{5/6} \quad (4)$$

From potential-step chronoamperometry at the stationary electrode in Me_2SO (potential step from 0.2 to 0.9 V; time greater than 10 s), D_{Me_2SO} for a 1 mM NADH solution is calculated to be $(0.9 \pm 0.1) \times 10^{-6}$ cm^2 s^{-1}. Since D_{H_2O} was found to be $(2.3 \pm 0.1) \times 10^{-6}$ cm^2 s^{-1}, the calculated $i_{p(Me_2SO)}/i_{p(H_2O)}$ of 0.45 ± 0.08 is comparable to the experimental value of $0.35 + 0.02$ and indicates lack of a marked difference in solvation of NADH between Me_2SO and water as solvents, at least in respect to mobility.

Mechanistic Deductions and Interpretations

NADH is produced on reduction of NAD^+ in a one-step process enzymatically (eq 5) and in a two-step process electrochemically (eq 6). 1,4-NADH, which is the sole product enzymatically and

$$NAD^+ + H^+ + 2e^- \overset{\text{enzyme}}{\rightleftharpoons} NADH \quad (5)$$

$$NAD^+ + e^- \underset{\text{ca. -1.0 V}}{\overset{\text{electrode}}{\rightleftharpoons}} NAD\cdot \xrightarrow[\text{ca. -1.6 V}]{+H^+, e^-} NADH \quad (6)$$

the principal product electrochemically (some 1,6-NADH is also formed), is oxidized to NAD^+ in a single step enzymatically and electrochemically (at ca. 0.5 V). Most chemical oxidations of NADH have been explained—similarly to the enzymatic oxidations—in terms of direct transfer of a hydride ion from the dihydropyridine to the oxidizing agent.

According to an ECE mechanism, the first step would consist of an irreversible heterogeneous electron transfer, yielding the cation radical $NAD{\cdot}H^+$:

$$NADH \xrightarrow{E_1\,(\beta)} NAD{\cdot}H^+ + e^- \quad (7)$$

The large activation energy may be due to the fact that, before 1,4-NADH can lose an electron, it must undergo a rearrangement. For example, in order to justify the experimental results, we may consider reaction schemes such as Scheme I, where R represents adenosine diphosphoribose (ADPR), since the amide group may possibly be involved in a transitory stage of the oxidation process as suggested by the fact that only 1,4-NADH is enzymatically active. The enol form may also be the electrochemically oxidizable form since orthoquinones covalently bound to carbon electrodes catalyze the electrochemical oxidation of NADH as well as the electrochemical oxidation of an ene–diol such as ascorbic acid.[20]

The second step would be a first-order deprotonation reaction to produce the neutral radical NAD· (see eq 9a and 9b). This

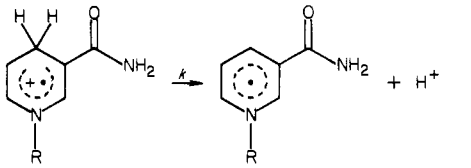

(9a)

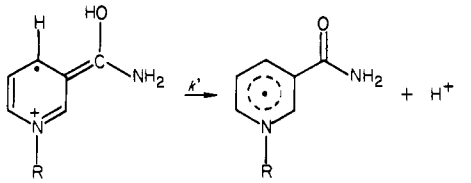

(9b)

$NAD{\cdot}H^+$ NAD·

reaction may be considered as practically irreversible since the neutral radical, due to its aromatic ring, is probably much more stable than the cation radical. This assumption is in good agreement with the cathodic behavior of NAD^+, i.e., the absence of an $E_{1/2}$ shift with pH for NAD^+ reduction wave I and the occurrence of only a slight $E_{1/2}$ shift with pH for wave II show that the protonation of NAD· is neither easy nor rapid.[21,22] The absence of pH dependence for the voltammetric results reported in the present paper (at least with carbon electrodes) also supports the irreversibility of reaction 9a or 9b.

The third step would be a second heterogeneous electron transfer as in eq 10. This electron transfer is reversible and $E_2°$ is ca.

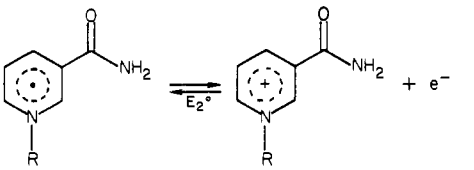

(10)

NAD· NAD^+

−1.0 V.[2,22,23] NAD· dimerizes very rapidly[22,23] but, since the dimer is electrochemically oxidized at ca. −0.4 V,[6,12,22] it would be ox-

(19) P. Delahay, "New Instrumental Methods in Electrochemistry", Wiley-Interscience, New York, 1954, p 230.

(20) D. Chi-Sing Tse and T. Kuwana, *Anal. Chem.*, **50**, 1315 (1978).

(21) K. S. V. Santhanam and P. J. Elving, *J. Am. Chem. Soc.*, **95**, 5482 (1973).

(22) M. A. Jensen, Ph.D. Thesis, The University of Michigan, Ann Arbor, 1977.

(23) C. O. Schmakel, K. S. V. Santhanam, and P. J. Elving, *J. Am. Chem. Soc.*, **97**, 5083 (1975).

Table II. Effect of Rotation Rate on the Oxidation of NADH at a Glassy Carbon Rotating Disk Electrode[a]

f, rps	ω, rad s^{-1}	i_l/AC,[b] μA cm^{-2} mM^{-1}	$i_l/AC\omega^{1/2}$	n_{app}/n[c]
2.5	15.7	174 ± 4	37 ± 1	2.0
5	31.4	213 ± 5	38 ± 1	2.0
10	63	285 ± 8	36 ± 1	1.90 ± 0.05
20	126	380 ± 20	34 ± 2	1.8 ± 0.1
40	251	490 ± 50	31 ± 3	1.6 ± 0.2
80	502	600 ± 60	27 ± 3	1.4 ± 0.2

[a] Electrode (Tacussel GCE) covered with adsorbed NAD^+. Background: 0.5 M KCl and 0.05 M phosphate buffer; pH 7. Data given are in each case the mean and standard deviations for three measurements. [b] Electrode area $A = 0.050$ cm^2; NADH concentration $C = 1$ mM. [c] Definitions of n_{app} and n are given in the text.

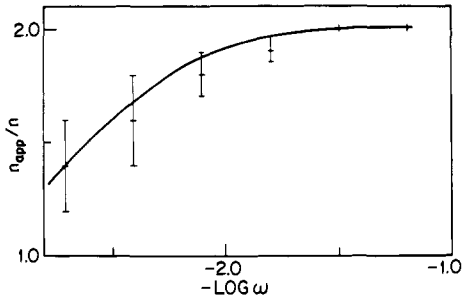

Figure 4. Effect of angular velocity, ω, on the oxidation of NADH at a rotating covered GCE ($n = 1$ and $n_{app} = i_l/19AC\omega^{1/2}$). Experimental conditions are given in Table II. Experimental margins of error are indicated for each measurement. The continuous curve was computed from the appropriate equation in ref 24b for $k = 50$ s^{-1}.

idized to NAD^+ at potential E_1 (ca. 0.5 V).

Deprotonation Rate Constant of the Cation Radical. For sweep voltammetry, the current function vs. log $(RTk/\beta Fv)$ working curve given in the literature[13] enables determination of k for reaction 9 and computation of the current function vs. log v curve for this k value as drawn in Figure 1, for which the theoretical curve fits the experimental plot within the margin of error.

For potential-step chronoamperometry, the theoretical i vs. $t^{-1/2}$ curve,[15] computed for the value of k determined by sweep voltammetry, also fits the experimental plot within the margin of error (Figure 3).

In order to confirm the occurrence of an ECE mechanism and to obtain a measurement of k by a third approach, we did rotating disk electrode (RDE) experiments over a range of angular frequency, ω, by using a commercially available GCE covered with adsorbed NAD^+ ($\omega = 2\pi f$, where f is the rotation in revolutions per second, rps). Above 20 rps, the anodic wave becomes less well-defined due to a positive shift of $E_{1/2}$ and to a decrease in the slope of the wave. Despite the resulting decrease in accuracy of determination of i_l, it is apparent that the ratio of $i_l/AC\omega^{1/2}$ decreases with increasing f above 10–20 rpm (Table II). If the value of 38 for $i_l/AC\omega^{1/2}$ at low f is assumed to correspond to a 2e diffusion-controlled process, the ratio of n_{app}/n can be plotted vs. $-\log \omega$ (Figure 4) for $n = 1$ and $n_{app} = i_l 19AC\omega^{1/2}$. Use of the equations developed for the application of the RDE to the study of ECE mechanisms[24] allows the calculation of k from such a plot.

Values calculated for k for various electrodes and background electrolytes are summarized in Table III; the values obtained in aqueous media with carbon electrodes covered with adsorbed NAD^+ are somewhat greater than those for the platinum electrode. The result obtained at the rotating GCE is in agreement with those obtained by linear sweep voltammetry and potential-step chronoamperometry at stationary electrodes.

At GCE, in pH 7.1 aqueous medium, k at 5 °C is approximately one-fourth of that at 25 °C. Such a twofold increase in rate constant for each 10 °C interval confirms the presence of a chemical-limiting step (activation energy = ca. 60 kJ mol^{-1}).

Table III. Values Calculated for k for the Reaction[a] $NAD{\cdot}H^+ \xrightarrow{k} NAD\cdot + H^+$

electrode	bkgd and buffer	pH	k, s^{-1}
GCE[b]	0.25 M Na_2SO_4 or 0.5 M KCl; 0.05 M Tris or phosphate	6–10	60 ± 30[f,i] 60 ± 30[g,i]
GCE[c]	0.5 M KCl; 0.05 M Tris	7	50 ± 30[h,j]
GCE[b]	0.1 M Bu_4NClO_4 in Me_2SO		8 ± 4[f,j] 7 ± 4[g,j]
PGE[d]	0.5 M KCl; 0.05 M Tris	7.1	20 ± 10[f,k]
PE[e]	0.5 M KCl; 0.005 M Tris	7.1	2 ± 1[f,k]

[a] NADH concentration = 1 mM. [b] Stationary CG-2 electrode covered with adsorbed NAD^+. [c] Rotating commercial electrode covered with adsorbed NAD^+. [d] Stationary electrode covered with adsorbed NAD^+. [e] Stationary electrode without preparation or pretreatment. [f] Based on the sweep voltammetric relation $RTk = \beta Fv_0$ (cf. Figure 1). [g] Based on the chronoamperometric i vs. $t^{-1/2}$ curve (cf. Figure 3). [h] Based on the effect of electrode rotation rate (cf. Table II). [i] Mean and standard deviations for 10 experiments. [j] Mean and standard deviations for 3 experiments. [k] Mean and standard deviations for 5 experiments.

Reaction Pathway. The irreversibility of the first electron transfer may well be the major cause of the large overpotential for the electrochemical NADH oxidation (ca. 0.5 V) when being compared to the enzymatically determined oxidation potential (ca. −0.56 V at pH 7).

The following processes may also be considered as component steps in the reaction path:

(a) NADH diffuses toward the electrode through an adsorbed NAD^+ (or tetraalkylammonium ion) layer. The electron transfer would then occur at the electrode surface but the progression of NADH toward that surface would be at least partially hindered and rate limited, since NADH would have to advance through holes in the adsorbed layer.

(b) Electron transfer from NADH to the electrode occurs through an adsorbed layer, e.g., NADH exchanges the electron with an adsorbed NAD^+ which, in turn, exchanges the electron with the electrode; in this sequence, the adsorbed NAD^+ functions as a mediator.

In these latter eventualities, the presence of NAD^+ at the interface may control at least part of the reaction sequence. For example, at the platinum electrode, where adsorption of NAD^+ is not detected, oxidation occurs approximately at the same potential as at a carbon electrode covered with adsorbed NAD^+ but β is greater (Table I).

As NAD^+ is known to form charge-transfer complexes and to exchange protons with a reduced nicotinamide moiety,[25] it may well be that adsorbed NAD^+ favors a pathway according to the scheme of reaction 8b while the pathway according to the scheme of reaction 8a is favored at the platinum electrode whose surface is not covered with adsorbed NAD^+. Then, the deprotonation rate constant of the cation radical would be apparently dependent on the electrode material as a result of the fact that the heterolytic cleavage of an oxygen–hydrogen bond (reaction 9b, rate constant k') is expected to be faster than the heterolytic cleavage of a carbon–hydrogen bond (reaction 9a, rate constant k). The differences in k values reported in Table III could then be justified since these values are of the same order of magnitude for electrodes covered with adsorbed NAD^+ in aqueous media while the value found for k with the platinum electrode in the same media is smaller by at least 1 order of magnitude. The intermediate value found in Me_2SO with an electrode covered with adsorbed NAD^+

(24) (a) P. A. Malachesky, L. S. Marcoux, and R. N. Adams, *J. Phys. Chem.*, **70**, 4068 (1966); (b) S. Karp, *J. Phys. Chem.*, **72**, 1082 (1968).

(25) J. Ludowieg and A. Levy, *Biochemistry*, **3**, 373 (1964); G. Blankenhorn, *Eur. J. Biochem.*, **67**, 67 (1976).

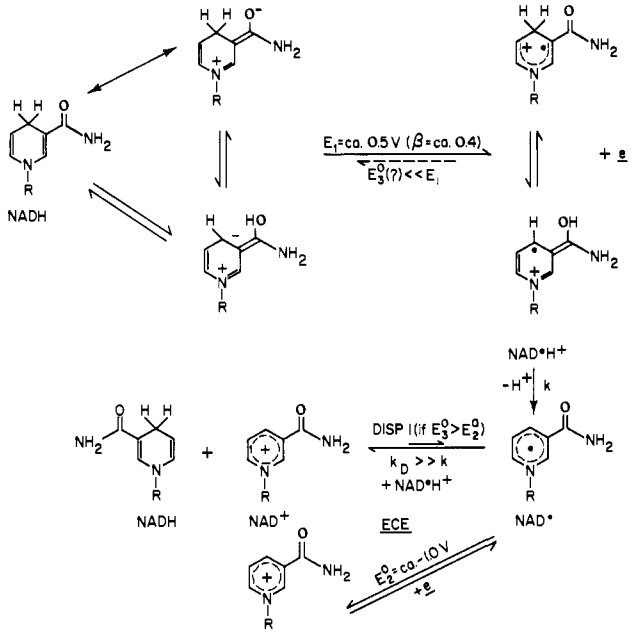

Figure 5. Reaction path for the electrochemical oxidation of NADH: E_1 is the oxidation potential of NADH to NAD·H$^+$ (eq 7 and 8); $E_2°$ is the reversible potential for the NAD$^+$/NAD· couple (eq 10); $E_3°$ is the reversible potential for the NAD·H$^+$ couple; k is a deprotonation rate constant (eq 9); k_D is a disproportionation rate constant (eq 11). NAD$^+$, NAD·, and NAD·H$^+$ can exist in resonant forms.

could result from a slight difference in solvation.

It should be noted that the pH range involved (pH 6–10) is one in which the dissociated phosphate groups in NADH and NAD$^+$ may serve as bases for proton supply and removal. The deprotonation rate may well be pH dependent at pH less than 6 where the hydrogen ion activity in the bulk solution is appreciable.

In respect to the second electron transfer, a disproportionation involving cation radical NAD·H$^+$ and neutral radical NAD· may also occur since the observation of a 2e process may be explained as well by the occurrence of the solution electron transfer (eq 11, half-regeneration reaction), as soon as the condition $E_3° > E_2°$ is fulfilled, where $E_3°$ is the reversible potential for redox couple NAD·H$^+$/NADH. As this couple does not exhibit reversible electrochemical behavior, experimental information on the value of $E_3°$ is lacking. However, it is reasonable to assume that the cation radical is easier to reduce than the neutral radical. As deprotonation reaction 9a or 9b is not very fast, it would probably remain the rate-limiting step, i.e., the disproportionation is more

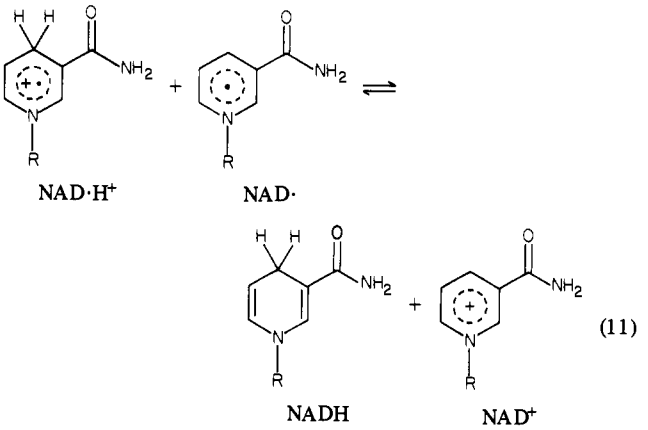

(11)

rapid than the deprotonation and the latter controls the extent to which the disproportionation occurs. The resulting mechanism has been termed a DISP 1 mechanism;[13,26] when the chemical reaction preceding the disproportionation is irreversible as assumed in the present paper, it has been established that ECE mechanisms do not occur under conditions where they can be directly characterized by electrochemical kinetic techniques and that, under these conditions, the DISP 1 mechanism will predominate.[27] However, the working curves for both sweep voltammetry[13] and potential-step chronoamperometry,[15,28] which allow the determination of k for an ECE mechanism on the one hand and for a DISP 1 mechanism on the other hand, give values which are close together and cannot be distinguished when the experimental margin of error is taken into account.

Figure 5, then, represents the state-of-the-art knowledge concerning the electrochemical oxidation of NADH. NADH is irreversibly oxidized (loss of an electron with a transfer coefficient of ca. 0.4) to produce a cation radical NAD·H$^+$, which deprotonates to produce a neutral radical NAD·. Since NAD· forms a reversible couple with NAD$^+$ at about −1 V,[23] it is immediately oxidized to NAD$^+$ at the electrode surface at the positive potential involved (ca. 0.5 V) or, in solution, exchanges an electron with the cation radical.

Acknowledgment. The authors thank the National Science Foundation, which helped support the work described.

(26) L. Nadjo and J. M. Saveant, *J. Electroanal. Chem.*, **33**, 419 (1971).
(27) C. Amatore and J. M. Saveant, *J. Electroanal. Chem.*, **86**, 227 (1978).
(28) D. H. Evans, T. W. Rosanske, and P. J. Jimenez, *J. Electroanal. Chem.*, **51**, 449 (1974).